Probing thin-film $YBa_2Cu_3O_{7-\delta}$ superconductors by second-harmonic generation with the use of femtosecond laser pulses

Jane K. Rice, S. W. McCauley,* and A. P. Baronavski
Chemistry Division, Code 6111, Naval Research Laboratory, Washington, D.C. 20375

J. S. Horwitz and D. B. Chrisey
Condensed Matter and Radiation Sciences Division, Code 6674, Naval Research Laboratory, Washington, D.C. 20375
(Received 6 July 1992; revised manuscript received 9 October 1992)

High-temperature superconducting thin films of $YBa_2Cu_3O_{7-\delta}$ are examined by measuring the second-harmonic generated (SHG) signal from an incident 60-fs laser pulse of 2.0 eV (620 nm) in air at room temperature. As oxygen stoichiometry is varied ($0.00 < \delta < 0.50$), large changes in the SHG intensity are observed. The oxygen content of the films is independently determined by measuring (i) the *c*-axis lattice parameter derived from x-ray diffraction and (ii) the stoichiometry of the films determined by elastic backscattering spectrometry. We report a negative correlation of the SHG intensity with the *c*-axis parameter indicating that a known compression of the *c* axis leads to a *larger* SHG signal. An additional experiment in which the SHG intensity is monitored as a function of temperature (300–20 K) in vacuum is performed. A gradual increase of ~50% in the SHG intensity is observed as the temperature is lowered, which can also be correlated to a decrease in the length of the *c*-axis parameter. Other experiments including rotation anisotropy and polarization of the incident and analyzer beams are also discussed.

I. INTRODUCTION

Second-harmonic generation (SHG) from surfaces has proven to be a highly informative probe of interfacial boundaries. Initial studies of the nonlinear response from a metal surface have been followed by the application of SHG to gain information concerning molecular orientation, concentration, and species identification on surfaces.[1–3] One of the problems in these studies has been damage to the surface under study. The damage results from the high peak powers (>10 MW/cm^2) necessary to obtain reasonable signals. For nanosecond lasers, this power corresponds to >10 mJ/cm^2, which is enough to cause local melting of the surface or, at the very least, disruption of the more labile bonds. For this reason, femtosecond lasers possess a real advantage over other laser sources. Their short pulse widths ($\sim 100\times10^{-15}$ s) and mean intensities of 10 MW/cm^2 can easily be attained with corresponding fluences of only 10 μJ/cm^2. Therefore, surface damage can be eliminated entirely in most cases and several surface characteristics can be probed.

We address two important aspects of surface diagnostic experiments on thin-film high-temperature superconductors (HTSC's). First, the use of femtosecond pulses to produce SHG can provide a *nonintrusive* and *nondestructive* means of probing these materials.[1,3] Second, since the first technological application of HTSC materials has been as thin films, a technique which has the potential to monitor the chemical structure or free-electron density near the surface (within ~500 Å) is extremely desirable. SHG from several HTSC materials has been reported in which absolute intensities of SHG and third-harmonic generation (THG) have been examined.[4] The SHG signal intensity is reported to be larger from $YBa_2Cu_3O_{7-\delta}$ (YBCO) than from silicon.[4] SHG has also been reported from the $La_{1.8}Sr_{0.2}CuO_4$ superconductor.[5] These studies were brief with little characterization of the superconducting materials.

Several studies have shown the importance of understanding oxygen deficiencies in the crystal lattice of YBCO thin films. The highest critical temperatures (T_c's) for these films are attained only for a specific stoichiometry of oxygen.[6–8] A compositional change from $\delta=1$ to 0 for $YBa_2Cu_3O_{7-\delta}$ affects the crystal structure, e.g., lattice parameters of the film, and varies the electrical properties from insulating to superconducting. Many aspects of the influence of the structural parameters on the electrical properties are still not well understood. The data presented here demonstrate that optical measurements using SHG can identify oxygen deficiencies in the films and may help determine why the electronic properties of the films are affected so strongly.

The origin of SHG from a metal surface is due to the dipole term of the susceptibility, which is nonzero at the interface of a centrosymmetric material.[1–3] This is defined as a material in which an inversion through the center of the unit cell leads to an identical species. The intensity of the reflected SHG from excitation by a plane wave of frequency ω and polarization $\mathbf{e}(\omega)$ is

$$I(2\omega)=\frac{32\pi^3\omega^2\sec^2\theta_{2\omega}}{c^3\epsilon_1(\omega)\epsilon_1^{1/2}(2\omega)}|\mathbf{e}(2\omega)\cdot\chi^{(2)}_{s,\text{eff}}\cdot\mathbf{e}(\omega)\mathbf{e}(\omega)|^2I^2(\omega)\ , \quad (1)$$

where $\theta_{2\omega}$ is the angle of incidence relative to the surface normal and $I(\omega)$ is the pump intensity. The symbols $\mathbf{e}(\omega)$ and $\mathbf{e}(2\omega)$ are related to the unit polarization vectors by the Fresnel coefficients. The effective nonlinear susceptibility $\chi^{(2)}_{s,\text{eff}}$ at the surface includes a surface term $\chi^{(2)}_s$ and bulk magnetic dipole contributions.[9] The tensor $\chi^{(2)}_{s,\text{eff}}$ simplifies to three nonzero elements for an isotropic medium.

The YBCO crystal structure is centrosymmetric. The thin films used in this study have near-single-crystal structure and are centrosymmetric. Consequently, the material has no electric dipole bulk term, except that generated from possible defects in the film. The SH tensor elements have not been calculated for an orthorhombic crystal but based on the terms from the simple-cubic case, p-polarized output contains contributions from all the $\chi^{(2)}_{s,\text{eff}}$ elements; therefore, surface and bulk effects cannot be separated.[2,10] Estimates of the relative contributions of bulk and surface terms have been made for various materials.[10] Conductors or materials with high dielectric constants will typically have a much larger surface term. Semiconductors will, in general, have surface and bulk term intensity on the same order. Insulators will have a lesser surface term. The HTSC's used here can be thought of as low current carrying metals having no gap in the normal state, even though they are made of oxide material which is otherwise considered insulating. In addition, YBCO has a small bulk magnetic term. Based on this, we suggest that the surface term may be on the same order as, or larger than, the bulk term in these materials. A complete examination of the origin of the SHG intensity reported here can provide a way to monitor changes in the HTSC thin films, at the least, and may help in determining the parameters important to the superconducting state.

II. EXPERIMENT

The experiments reported here were carried out in three stages. At first, preliminary SHG measurements were made on several YBCO films. The films were 400 to 6000 Å thick, they were deposited on MgO⟨100⟩ or $SrTiO_3$⟨100⟩ substrates, and they had T_c's of ~84 K. In addition, one oxygen deficient film ($T_c = 57$ K) was examined and yielded a much lower SHG intensity than films of $T_c \sim 84$ K. These initial measurements were followed by a pilot study of four films prepared under controlled conditions and characterized for film structure by x-ray diffraction (XRD), atomic composition by elastic backscattering spectrometry (EBS), and dc transport indicated by T_c and J_c ($B = 0$, 77 K). These films were studied using SHG and reflection measurements. Two of the films had a $T_c \sim 90$ K which we will refer to as "standard" (labeled $S1$ and $S6$) and two were oxygen deficient films (labeled $D1$ and $D6$). One pair of standard and oxygen deficient films was grown on the MgO⟨100⟩ substrate and the other on $SiTiO_3$⟨100⟩. The same SHG intensity dependence on the oxygen content was observed. Thirteen additional films were added to the study. Eight were deposited on MgO and five on $SrTiO_3$. Six were 6000 Å thick and seven were 3000 Å thick. Six were standard films and seven were oxygen deficient. These were made six months after the four pilot films with the exception of $D9$, which was made nine months later. Characterization of these films (including EBS on $SrTiO_3$ substrates) was done after the SHG measurements were completed. This accounts for the 17 films which provide the statistical basis for the film parameters and SHG correlations presented here.

A. Film preparation

The YBCO films were prepared by pulsed laser deposition.[11] The output of a Lambda Physik EMG-315 KrF excimer laser operated at 248 nm with an energy of 125 mJ per pulse was focused to an energy density of ~2 J/cm^2 onto a rotating target of bulk superconducting material. The vaporized material was deposited onto a heated substrate (750 °C) positioned ~4 cm from the target. Films were typically deposited in a high background pressure of O_2 (300 mTorr). Following deposition, films were cooled in 1 atm of O_2 to yield standard YBCO films with $T_c \sim 90$ K or films were cooled in 300 mTorr of O_2 to yield oxygen deficient films with $T_c \sim 60$ K.[12]

Characterization of the films was carried out using standard techniques. Transition temperatures were determined from ac magnetic susceptibility measurements.[13] Films were characterized by XRD in the standard $\theta/2\theta$ mode using Cu(K_α) radiation. The c-axis lattice parameter was calculated from the 00,10 reflection. These XRD studies indicated that the YBCO films were oriented with the c axis normal to the substrate and with the exception of film number $D9$, the films displayed narrow rocking curve widths of $0.15 < \Gamma < 0.28$ (for the 002 reflection). The lower limit for Γ of 0.15 represented the experimental resolution of the instrument. Oxygen stoichiometry and film thicknesses were measured using EBS with 6.2-MeV He^{+2} for those films deposited on $SrTiO_3$. Other film thicknesses were estimated from the deposition time.

B. Optical measurements

The apparatus used to make the SHG measurements at room temperature in air consisted of a femtosecond laser with pulses of ~60 fs duration and 4.5 μJ/pulse, a sample mounting station, a monochromator, and a photon counting system. The femtosecond laser pulses were produced by a colliding pulse mode-locked (CPM) laser (Clark, Inc.) which was amplified by a 350-Hz Lambda Physik (LPX-240i) excimer laser operating at 351 nm with 10 mJ of energy pumping a modified bow-tie amplifier (Clark, Inc). The output of the laser was horizontally polarized. The laser beam impinged on vertically mounted films on a rotating stage which was placed at a 45° angle to the incident beam. The reflected beam passed through a polarization analyzer and several glass filters (UG-11 and 7-54), which transmitted the second harmonic at 310 nm and blocked the fundamental at 620 nm, onto the open slits of a $\frac{1}{4}$-m Jarrell-Ash monochromator. A photomultiplier tube (PMT) (1P28) was used for light detection and the SHG signal was monitored by a photon counter (Stanford Research Systems 9400). For

most of the results presented, multiple photon events were counted by scanning the discriminator value in 3.2-mV increments. The threshold value of 3.2 was determined by a test of the PMT output distribution as a function of discriminator voltage. The number of counts at the first discriminator value of 3.2 mV represents a single count of all events whether they are single- or multiple-photon events. The discriminator voltage was then increased to 6.4 mV and the counts here represent the number of events generated from two simultaneous photons. The discriminator value was increased in 3.2-mV increments until the total number of counts (sum of all counts at all previous discriminator voltages) at that voltage was $<2\%$ of the value at the lowest (3.2 mV) discriminator voltage. Multiple-photon events were counted in this manner for all the data presented here except in a study of the SHG variation over the surface of the film. This is noted in the text. In all cases, a background signal was collected following each SHG measurement by using a blue cutoff filter between the film and the polarization analyzer. The dark counts associated with this measurement constituted less than 10% of the weak SHG signals and were subtracted from the SHG intensity measurement.

The SHG was examined under different incident and reflected polarization combinations, i.e., *s,s*; *s,p*; *p,s*; and *p,p*. In these cases a polarization rotator was placed in the laser beam before the film to rotate the polarization from a *p* incident polarization to an *s* incident polarization.

The temperature-dependence measurements (300–20 K) were collected by mounting the films in a Displex cryostat in a vacuum of 5×10^{-6} Torr. The incident laser light was attenuated by the entrance and exit windows on the cryostat and the effect was compensated for by slightly focusing the beam onto the sample with a 0.5- or 1-m lens. The polarization combination used was *s,p*. In this measurement, a Cu vapor laser was used to amplify the CPM laser and its repetition rate was 6000 Hz. Because of the high repetition rate, a picoammeter was used to detect the output from the PMT.

III. RESULTS

Two types of measurements have been collected from the HTSC thin films: the optical measurements related to the SHG signal which are presented here and those which independently characterize the electrical transport and crystallographic structure of the films discussed previously. The optical measurements can be divided into those which test the SHG signal characteristics such as the power dependence, polarization dependence, and rotational anisotropy, and those which test characteristics of the films such as the SHG intensity variations over the surface of a film and the comparison of the SHG intensity from a standard film to an oxygen deficient film.

A. Power dependence

The power dependence of the SHG from a standard YBCO sample was examined. A fit to the equation of $I_{\mathrm{SHG}} \propto I^{n}_{\text{laser power}}$ yields a power dependence of $n=2.8\pm0.2$. To obtain this dependence, the intensity of the SHG was normalized to the reflection of the fundamental beam from the film surface. Without normalizing to the reflection, n is much greater than 2.8 indicating that the reflection does not vary linearly with power. This may be due to changes in the optical penetration depth in the film as the laser power is changed. Because the power dependence from YBCO is somewhat higher than expected, the power dependence from Si(100) was done with the result $n=1.7\pm0.15$. This measurement, including the same normalization to reflection, has the value 2 with 90% certainty. We are continuing to investigate the source of the high value from the YBCO film.

B. Polarization dependence

The intensity of the SHG as a function of the incident and exit polarizations cannot determine whether the SHG signal originates predominantly from the surface or the bulk, however, it has been shown in some cases that *s*-polarized output[2] is stronger when the SHG emanates from the surface. In the data presented here on the standard YBCO thin film, the most intense SHG is produced in the *s,p* and *p,p* configurations. In fact there is at least a factor of 5 lower intensity from the *s,s* and *p,s* configurations. To make the comparison between the relative intensity of *s,p* and *p,p* polarizations, the incident laser beam was attenuated with the *p,p* configuration to match the maximum intensity in the *s,p* configuration. The relative *s,p* intensity is 1 ± 0.2 compared to a *p,p* intensity of 0.6 ± 0.2. The background or zero values are on the order of 10 counts/s and are about 2% of the *s,p* intensity in counts/s. Much of the data reported here have been collected with *p,p* polarization. The exceptions are a few of the diagnostic tests, the film variation test, and the temperature dependence.

C. Rotational anisotropy

Single-crystal metals and semiconductors exhibit a variation in the intensity of SHG as the solid-state surface is rotated through 360° relative to an incident beam.[14,15] The pattern is related to the point group of the crystalline face. The presence of this characteristic pattern provides direct proof that the SHG signal monitored is generated on the material surface. Rotational anisotropy experiments were performed on Si(111), Si(100), and Si(110) as a test and results similar to those reported by Tom, Heinz, and Shen[15] were observed. This was followed by rotational anisotropy experiments on YBCO films deposited on MgO$\langle 100\rangle$. The films have the *c* axis perpendicular to the surface and the *a* and *b* axes parallel to the surface of the substrate. The *a* and *b* axis lengths are 3.856 and 3.870 Å, respectively. The in-plane orientation has been determined from XRD pole figure measurements on MgO. The deposited films show maxima at 45° and 90° for *a-b* misorientations, while on $SrTiO_3$ only 90° misorientations are observed. The results of the rotational anisotropy experiment presented here indicate no variation in intensity larger than 15% from these samples, which is on the order of the experimental error.

D. SHG variation over the film surface

The SHG signal was tested in ten random surface positions on several films. The measurement was made on two standard films ($S1$ and $S6$) and two oxygen deficient films ($D1$ and $D6$). A bar graph of this variation is shown in Fig. 1. The SHG is not normalized to the reflection in this case. The standard deviation of the SHG intensity from various locations on the film is $\sim\pm 15\%$ for both the standard and oxygen deficient films. We can conclude from this that uniformity of the standard and oxygen deficient films is similar. Multiple-photon events were not counted and so the ratio of the SHG intensity of standard to oxygen deficient films, which is ~ 2.0 from these four films, represents a lower limit of the ratio.

E. SHG from standard vs oxygen deficient films

The primary result of this paper is the observation that standard films have a significantly *larger* SHG than oxygen deficient films. Oxygen deficient films have lower T_c's and previous reports have determined a correlation between the T_c and the c-axis parameter.[12,16] As the oxygen stoichiometry decreases from 7 to 6.5, the c axis lengthens from 11.697 to 11.786 and the T_c decreases from 90 to 55 K.

1. Elastic backscattering

The oxygen stoichiometries, i.e., $7-\delta$, from the EBS measurements are given in Table I. The δ value was estimated from the oxygen atomic fraction. The uncertainty of the EBS measurement is estimated to be $\sim 20\%$, therefore, the measured values that are higher than the theoretical limit of 7.0 are within the estimated uncertainty. The mean value of the oxygen fraction is 7.2 ± 0.2 from the standard films and it is 6.5 ± 0.2 from the oxygen deficient films. This confirms that the films designed to be oxygen deficient are indeed that.

2. Film parameters

Seventeen samples were tested for linear correlations between the SHG optical measurement and the electronic properties of the films. Approximately half the films were deposited on MgO⟨100⟩ and the other half on $SrTiO_3$⟨100⟩. The lattice parameters of $SrTiO_3$ are better matched to the unit cell of the YBCO and may result in better growth characteristics which may be revealed in the SHG intensity from the film. Also, EBS can be used to independently measure the oxygen stoichiometry for films grown on $SrTiO_3$ (but not MgO), providing an independent measure of the oxygen deficiency. However, the $SrTiO_3$ substrate has a strong SHG signal of its own, whereas the MgO substrate has no SHG signal. For these reasons, both MgO and $SrTiO_3$ films were produced in nearly equal pairs.

Two different film thicknesses were examined: these were ~ 3000 and ~ 6000 Å. In addition, the thickness of the substrates (not thought to be important) was also varied between 0.25 and 0.5 mm. These parameters, the x-ray-diffraction parameters such as c-axis length, δ, and the rocking curve widths (Γ), the electronic properties such as T_c and J_c, the SHG intensity, and reflection for each film are given in Table II.

3. SHG correlations

A linear correlation matrix of the measured parameters is given in Table III. The two optically determined parameters are the SHG and the reflection parameter. The reflection parameter is simply the laser power which is reflected from the film divided by the incident laser power and is included and used as a normalization factor to account for minor variations observed in the surface optical quality of the films. The reflection is a bulk term and has a linear laser dependence, however, all of the SHG intensity comparisons between standard and oxygen

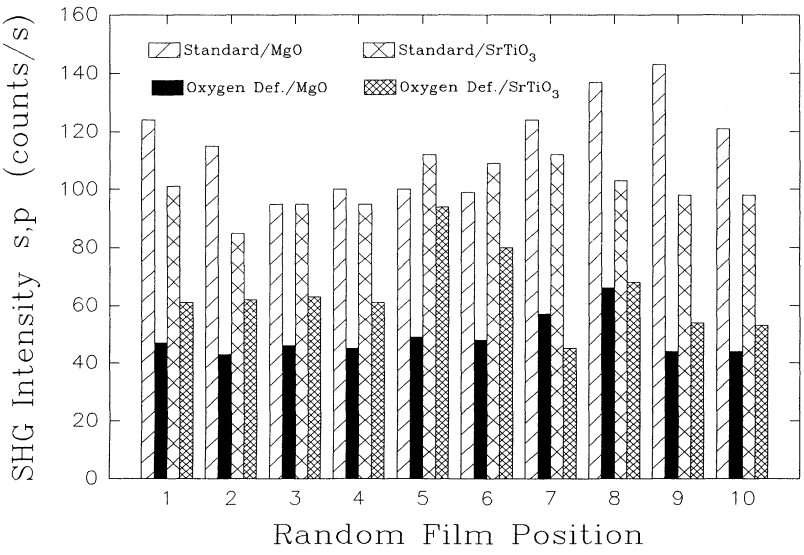

FIG. 1. SHG intensity in counts/s for the films $S1$ (standard/MgO), $D1$ (oxygen deficient/MgO), $S6$ (standard/$SrTiO_3$), and $D6$ (oxygen deficient/$SrTiO_3$) taken at ten different positions on the film. The SHG variation at each film position represents the error in the measurement plus any variation in the film surface. The effect of oxygen deficiency is much larger than these errors combined.

TABLE I. Elastic backscattering data.

Film identification	Thickness (10^{18} atoms/cm^2)	Calculated oxygen content ($7-\delta$)
*S*6	2.13	7.01
*S*7	2.71	7.15
*S*8	5.07	7.33
*D*6	1.82	6.37
*D*7	2.55	6.74
*D*9	1.80	6.52

deficient films were done with very little variation in laser power. The normalization to reflection is intended to provide a correction for small variations in the films. First, two separate correlation tables were calculated to compare the films deposited on MgO to those on $SrTiO_3$. No obvious differences were seen, therefore the two sets were combined for all comparisons shown here.

There are three high correlations shown in Table III. The highest, -0.92, indicates a negative correlation between the T_c values and the *c*-axis parameter; this correlation has been previously documented.[12,16] The other two correlations which can be analyzed together include that of the SHG to T_c which is 0.77 and the SHG to the *c*-axis length which is -0.65. If the sample *D*9 which also has a high rocking curve is not included, these values improve significantly to 0.82 and -0.77, respectively. These are relatively high correlations which link an optical measurement from the surface to the T_c.

Several other conclusions can be drawn from the correlation matrix. Film thickness does not correlate with the SHG. The rocking curve width (Γ) is somewhat correlated (0.33) to the *c*-axis parameter which indicates that broader curves are seen with a longer *c* axis. The rocking curve is not correlated with the SHG (0.18). The reflection measurement is somewhat correlated with the SHG (0.28) and the *c*-axis parameter (0.30). The correlation of the reflection with Γ (0.60) is due only to sample *D*9; this correlation is -0.21 for the other 16 samples.

4. *Multiple correlation analysis*

Further statistical analyses were done to determine if multiple correlation would improve the correlation between the SHG and the electronic parameters. These results are shown in Table IV. The first column is the coefficient of multiple (linear) correlation or the *R* coefficient. It is a correlation value between 0 and 1 which is calculated for the dependent variable labeled *Y* in column 2 and is correlated with several independent variables labeled X_n. By examining the *R* coefficient, we can determine the best combination of variables relevant to the SHG signal. We find a better *R* coefficient (0.89) when correlating SHG with both reflection and T_c. This is significantly better than the single correlation of SHG with T_c of 0.77 shown in Table III. The addition of the *c*-axis parameter and the rocking parameter do not im-

TABLE II. SHG intensities and characterization measurements on $YBa_2Cu_3O_{7-\delta}$ thin films.

Film identification	SHG[a]	Substrate	T_c (K)	ΔT[b]	J_c (MA/cm^2 at 77 K)	*c* axis (Å)	$7-\delta$[c]	Γ[d]	Reflection[e] (I_{out}/I_{in})	Estimated film thickness[f] (Å)	Measured film thickness[g] (Å)	Substrate thickness (mm)
*S*1	415	MgO	89.6	0.3	3.14	11.691	6.94	0.191	0.031	3000		0.50
*S*2	975	MgO	89.2	0.3	3.4	11.694	6.92	0.150	0.046	3000		0.25
*S*3	772	MgO	89.7	0.4		11.697	6.90	0.234	0.044	3000		0.50
*S*4	458	MgO	89.3	1.7	2.4	11.694	6.92	0.230	0.031	6000		0.50
*S*5	811	MgO	90.7	0.6	2.2	11.697	6.90	0.241	0.038	6000		0.25
*D*1	47	MgO	62.	4.6		11.750	6.56	0.231	0.030	3000		0.50
*D*2	64	MgO	55.	2.8		11.786	6.33	0.150	0.049	3000		0.25
*D*3	123	MgO	69.	3.9		11.751	6.55	0.234	0.043	3000		0.50
*D*4	75	MgO	67.	9.2		11.755	6.53	0.274	0.038	6000		0.50
*D*5	100	MgO	75.	4.6		11.752	6.54	0.279	0.039	6000		0.25
*S*6	313	$SrTiO_3$	91.6	0.5	3.64	11.676	7.03	0.150	0.028	3000	2716	0.50
*S*7	685	$SrTiO_3$	90.5	0.9	2.85	11.690	6.94	0.150	0.054	3000	3455	0.50
*S*8	608	$SrTiO_3$	90.6	0.4	2.0	11.701	6.87	0.150	0.049	6000	6465	0.50
*D*6	77	$SrTiO_3$	65.	3.8		11.726	6.71	0.150	0.021	3000	2320	0.50
*D*7	162	$SrTiO_3$	62.	5.1		11.741	6.62	0.167	0.062	3000	3251	0.50
*D*8	71	$SrTiO_3$	53.	2.8		11.758	6.51	0.184	0.055	6000		0.50
*D*9	706	$SrTiO_3$	72.	1.6		11.760	6.49	0.646	0.087	2000	2295	0.50

[a]The statistical uncertainty of the photon counts is $\pm 5-8$ % at one location on the film and $\sim \pm 15$ % if several locations are probed; *p*,*p* polarization is used.
[b]Values quoted are the ΔT associated with a 10% to 90% change in an inductive signal as described in Ref. 13.
[c]Calculated using the *c*-axis values shown here and $7-\delta$ vs *c*-axis values from Ref. 12.
[d]The rocking curve obtained from XRD. Values at 0.150 represent the lower experimental limit.
[e]Ratio of the fundamental beam reflected divided by beam input with *p*,*p* polarization.
[f]Estimated from the deposition exposure time.
[g]Obtained from EBS measurement.

TABLE III. Correlation matrix of measured parameters.

	SHG	T_c	c axis	ΔT	Film thickness	Substrate thickness	Rocking curve	Reflection
SHG	1							
T_c	0.77	1						
c axis	−0.65	−0.92	1					
ΔT	−0.72	−0.68	0.66	1				
Film thickness	−0.10	0.07	−0.01	0.21	1			
Substrate thickness	−0.18	−0.11	0.02	0.01	−0.19	1		
Rocking curve	0.18	−0.09	0.34	0.08	−0.12	0.01	1	
Reflection	0.28	−0.21	0.36	−0.08	−0.21	0.20	0.60	1

prove the correlation. A plot of the SHG normalized to the reflection factor vs the oxygen content is shown in Fig. 2. The oxygen content is calculated directly from the c-axis parameter using the formula given in Ohkubo *et al.*[12]

5. *Plot of SHG as a function of oxygen deficiency, film thickness, and substrate*

Several comparisons are shown in Fig. 3 in a graph of SHG intensities related to film characteristics. All the films were normalized to reflection (given in Table II), the SHG includes multiple-photon events, and all the films indicate a very large difference in the standard : oxygen deficient film ratio. The comparison labeled 1 are results from the four films $S1$, $D1$, $S6$, and $D6$ (from left to right). These 3000-Å films were made about six months prior to the other films in the study. The films labeled 2 have identical (except for age) characteristics to those in 1. These are films $S3$, $D3$, $S7$, and $D7$. The films labeled 3 are deposited on MgO only ($S2$, $D2$ and $S5$, $D5$) and compare two 3000-Å films (left) to two 6000-Å films (right). The films in position 4 are four 6000-Å films ($S4$, $D4$ and $S8$, $D8$) and compare the MgO and $SrTiO_3$ substrates as in comparisons 1 and 2. The collective ratio of the SHG intensity of standard to oxygen deficient films is a factor of ~8. These comparisons illustrate that film thickness and type of substrate are not correlated with the SHG intensity.

F. Temperature dependence

A decrease in the temperature of the YBCO film yields a decrease in the volume of the unit cell, providing another way of shortening the c axis. The temperature dependence of the SHG signal from several standard samples and one oxygen deficient sample was investigated between 300 and 20 K to determine if any change in the intensity of the SHG signal occurs. A plot of the temperature dependence of a standard film is shown in Fig. 4. We find a large gradual increase in the SHG intensity from these samples as the temperature is lowered. The temperature dependence of the oxygen deficient sample shows an increase of ~50% compared with increases of about 70% from the standard samples investigated. For comparison, two other materials were tested in the same manner; these were Si(110) (a semiconductor) and a film of gold (a conductor). Increases of about 30% and 15% were seen from the Si(110) and the gold film, respectively. Since UHV conditions are not used in this study and no attempt is made to eliminate the adlayers present on the films, we conclude that there are at least several layers of adsorbates on the films at all times during the ramping of temperature. The data presented are not corrected for any effects of additional condensation on the surface as

TABLE IV. Coefficients of multiple correlation.

R Coefficient	SHG	Reflection	T_c	c-axis parameter	Rocking curve
0.89	Y	X_1	X_2		
0.85	Y	X_1		X_2	
0.89	Y	X_1	X_2	X_3	
0.89	Y	X_1	X_2	X_3	X_4

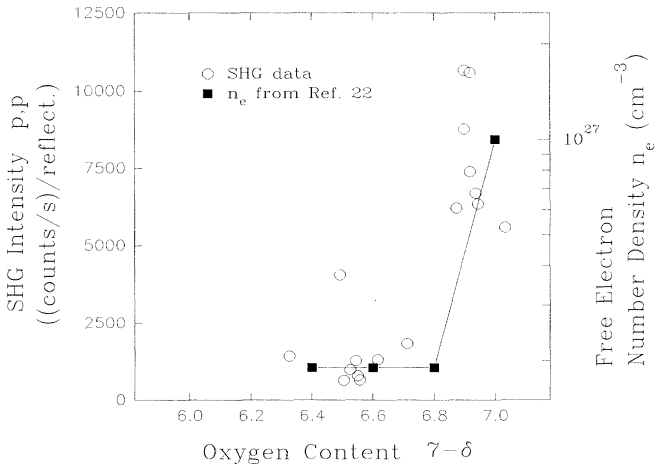

FIG. 2. The SHG intensity/reflection vs the oxygen content of the 17 films in the study. Also shown are the free-electron number densities at various oxygen stoichiometries taken from Ref. 22. These are arbitrarily scaled to the SHG data points.

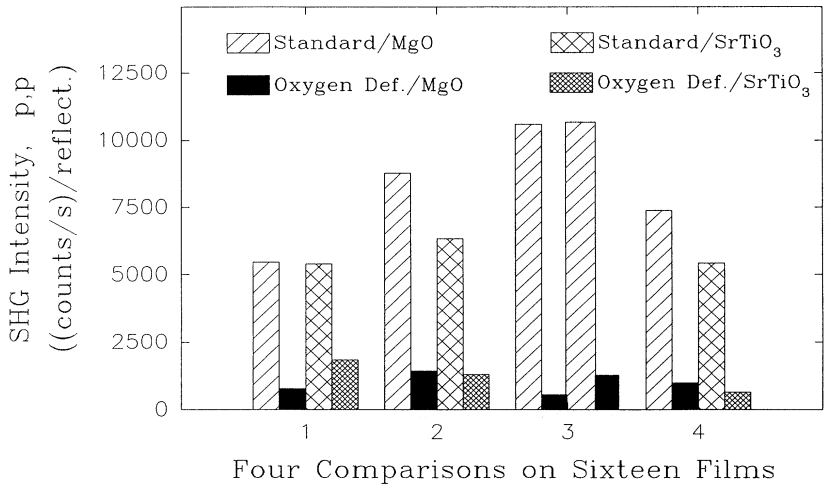

FIG. 3. SHG intensities from 16 films are shown. (1) Films which are standard and oxygen deficient on MgO and $SrTiO_3$, all 3000 Å thick, made six months prior to test. (2) Identical to (1), however, made a few weeks prior to test. (3) Films on MgO only, 3000 Å thick (two left) compared to 6000 Å thick (two right) of same age as (2). (4) Films 6000 Å thick of the same age as (2) and (3). See text for film identification.

the temperature is lowered, however, typically the most influential adlayers are the first one or two at the metal surface[17,18] which remain in place throughout the experiment. Also, no correction was made for possible changes in the reflection of the fundamental beam intensity as a function of temperature during this experiment.

IV. DISCUSSION

A. Is the SHG measurement of the c-axis parameter quantitative?

Using the c-axis dependence on temperature given in Horn *et al.*,[19] we calculate a correlation of 0.99 of SHG (from the temperature study) with c-axis length. A plot of the Horn *et al.*[19] data showing the c-axis length varying as a function of temperature is shown with the SHG data in Fig. 4. The plots are remarkably similar, showing the same inflection point near 100 K. An abrupt change in the c-axis parameter has been reported at the T_c by others.[20,21] We do not observe these changes under our experimental conditions.

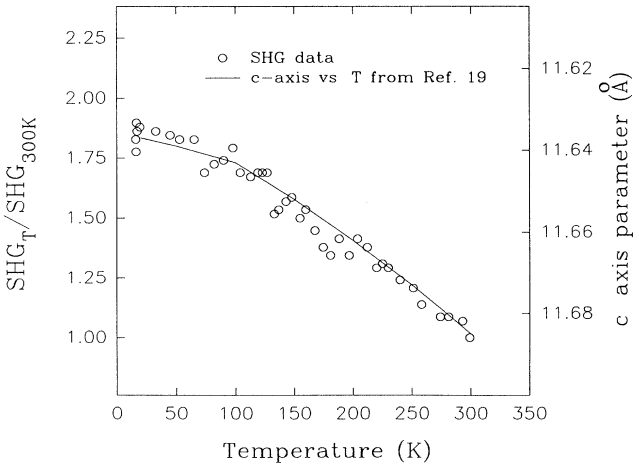

FIG. 4. SHG intensity from 300 to 10 K normalized to the 300-K value vs film temperature. (○) The data are taken from a standard film on MgO, 400 Å thick. Also shown is the c-axis compression as a function of temperature (——) from Ref. 19.

To determine whether the SHG responses to oxygen deficiency and temperature are comparable, we examine the factor by which the SHG increases and compare this to the c-axis change. In the case of temperature as the perturber of the c axis, a factor of ~ 1.6 is seen in SHG for a change in the c axis of 0.036 (for $300\ \text{K} > T > 100$ K). Using Fig. 1 data, which most closely resemble the experimental conditions, a factor of ~ 2.4 is seen in SHG (from MgO samples) corresponding to a change in the c axis of 0.059. These represent comparable ratios, therefore, the SHG intensity is sensitive to changes in the c-axis length caused by either oxygen deficiency or temperature and the magnitude of the SHG appears to be quantitative.

B. What is the origin of the SHG signal?

Authors of previous work on SHG from HTSC thin films have suggested several possible origins of the SHG signal. Because their intensity was found to be relatively high, Akhmanov *et al.*[4] suggested that SHG is due to a dipole term and possibly related to the presence of grains in the films. Although XRD indicated the perovskitelike structure, no transport measurements were reported, leaving questions about the composition, phase, and structure of the films. Golovashkin *et al.*[5] suggested that the SHG signals they observe (from bulk $La_{1.8}Sr_{0.2}CuO_4$) may be due to acentric clusters or a breakdown of the inversion symmetry; this is based on a comparison of the SHG intensity from $La_{1.8}Sr_{0.2}CuO_4$ and a typical ferroelectric, barium titanate. Again, there are questions about the composition and phase of the material used. In the studies reported here the SHG from the superconducting films ($T_c \sim 90$ K) is lower than that of silicon and all the data can be explained assuming a breakdown in the symmetry at the surface and not necessarily from a symmetry breakdown in the bulk material. However, at this time we have no way of determining the relative contributions from (i) surface, (ii) bulk: magnetic, and (iii)

bulk: dipole, due to material defects.

In a recent report, the radiative properties of oxygen rich and oxygen deficient YBCO films indicate a *c*-axis parameter dependence.[22] The normal reflectance and normal transmittance are measured at room temperature in the wavelength range from 1 to 100 μm. The reflection data from YBCO with an oxygen content of $7-\delta$ between 7.0 and 6.8 can be modeled using free-electron density and an electronic midinfrared absorption band. For films with lower oxygen content, phonon contributions are included. The magnitude of the reflection change in going from an oxygen content of $7-\delta=7.0$ to that of 6.6 is a decrease of $\sim 30\%$ with the addition of sharp structural features in the 1–100-μm spectral region.

Compression of the *c* axis in HTSC's does affect the free-electron density of the material.[19] This can be calculated using the equation

$$n_e=\omega_p^2\epsilon_0 m_e/e^2 , \tag{2}$$

where ω_p is the plasma frequency, ϵ_0 is the electric permitivity of free space (8.85×10^{-12} $C^2N^{-1}m^{-2}$), m_e is the electron mass (9.110×10^{-31} kg), and e is the electron charge (1.620×10^{-19} C).[22] The free-electron density changes in YBCO accompanying oxygen deficiency may explain the SHG intensities presented here. Using the plasma frequencies from Choi *et al.*,[22] which are 9600 ± 200 cm^{-1} for $7-\delta=7.0$, 4100 ± 200 cm^{-1} for $7-\delta=6.8$, and 4150 cm^{-1} for $7-\delta=6.6$, the free-electron density is added to Fig. 2 which compares the SHG intensity to *c*-axis parameter. The scale is arbitrarily chosen to best overlap the SHG data. The flat response of the SHG in the 6.4 to 6.8 range and the increase in going to 7.0 are consistent with the free-electron density calculation.

The predominant SHG intensity comes from the *p*-polarized output. We observed much weaker signals in the *s*-polarized output and under many laser power conditions the *s*-polarized output component is on the order of the background noise. A further study of the *s*- and *p*-polarized output components will not allow us to distinguish between bulk or surface origins, however a dual beam experiment may be helpful.[10] One experiment which may provide more information about the origin of the SHG would be to examine an untwinned, single crystal sample. Further comparisons among different superconducting materials of various free-electron densities may prove a connection between the SHG and the free-electron density.

C. Other possible sources of SHG

SHG has been demonstrated to be sensitive to a variety of surface structural features including surface roughness and material defects.[23] The effects of optical reflection from different films have been addressed by normalization to the reflection from each film and no large systematic differences were seen in the reflection of the standard vs the oxygen deficient films. However, it is possible that some surface feature and not free-electron density is contributing to or responsible for the SHG. The SHG signal is observed in an evacuated cold finger (5×10^{-6} Torr) at 300 K, however, this does not eliminate the possibility that the SHG is due to monolayers on the surface of the films. UHV studies are needed to see the effect of various monolayers. In this case the monolayers which adhere to the oxygen deficient films would be different or orient differently than those on standard films.

A number of structural changes in the film could contribute to the SHG signal. They must occur with both oxygen deficiency and temperature variation *or* separate explanations are necessary if a structural change is responsible for the SHG behavior. The range of δ values due to oxygen deficiency used in these experiments is not large enough to result in a phase change in the films. A change from orthorhombic to tetragonal at $\delta\geq0.6$ (Ref. 24) or 0.7 (Ref. 16) has been demonstrated, however, our values remain $\delta\leq0.6$ and indicate orthorhombic structure from XRD. Crystallographic structural changes are known to occur due to oxygen deficiency.[8] YBCO films with $\delta=0$ have ordered oxygen vacancies in the basal plane where linear (O-Cu-O) coordination have replaced square planar CuO_4, therefore the δ value can be related to the Cu ion charge.[25] For $\delta=0$, the average copper charge is 2.3, which is a (2:1) mixture of +2 and +3 valence states. There has been conjecture that the large range of mixed valence states in Cu in YBCO may be responsible for its high T_c.[26] When δ is greater than zero, the chains of $(\text{-Cu-O-})_n$ are defective and lead to lattice deformation.[27,28] Large oxygen deficiency has a pronounced effect on both the copper charge state and the nearest-neighbor coordination.[25] Samples with $\delta=0.5$ have an average Cu charge of 2.0.[29]

D. Is there a resonance at the fundamental wavelength?

One extension of this work would be to examine the effect of changing the fundamental wavelength. A resonance between the fundamental wavelength (or doubled wavelength) and interband transitions or surface states may enhance SHG intensity.[30,31] Resonances with adsorbates on the films may also enhance SHG intensity.[32] There are several reports of a weak transition from YBCO in the 1.9–2.0-eV energy range.[33–35] Our samples absorb throughout the visible region between 1.55 eV (800 nm) and 3.1 eV (400 nm) with a broad, small decrease in absorption near 2.0 eV (620 nm). Our spectra of standard and deficient films do not reveal any large differences, however, this does not eliminate the possibility that the standard films may be in resonance and the oxygen deficient films not.

V. CONCLUSIONS

SHG has been used to examine $YBa_2Cu_3O_{7-\delta}$ films as a function of oxygen stoichiometry ($7.0<7-\delta<6.5$) and

temperature (300–20 K). A correlation is observed between the c-axis lattice parameter and the SHG intensity. SHG intensity is significantly higher in those films with a compressed c axis. The SHG intensity correlates well with several electronic transport properties of the films and may be a nonintrusive and nondestructive way of monitoring the free electron density in the HTSC's.

ACKNOWLEDGMENTS

We thank Dr. D. C. Easter for his assistance in collecting the SHG data, Mr. V. Cestone and Dr. M. E. Reeves for the magnetic susceptibility characterization, and Dr. C. R. Gossett for the EBS measurements. Funding for this work was provided by the Office of Naval Research.

---

*Permanent address: Physics Department, California State Polytechnic University, Pomona, CA 91768.

[1]Y. R. Shen, Nature (London) **337**, 519 (1989).

[2]Y. R. Shen, *The Principles of Non-Linear Optics* (Wiley, New York, 1984), pp. 479–505.

[3]G. L. Richmond, J. M. Robinson, and V. L. Shannon, Prog. Surf. Sci. **28**, 1 (1988).

[4]S. A. Akhmanov, S. V. Govorkov, N. I. Koroteev, G. I. Petrov, I. L. Shumai, and V. V. Yakovlev, Bull. Acad. Sci. USSR Phys. Ser. **53**, 145 (1989).

[5]A. I. Golovashkin, V. S. Gorelik, A. M. Agal'tsov, O. M. Ivanenko, and K. V. Mitsen, Pis'ma Zh. Eksp. Teor. Fiz. **46**, 155 (1987) [JETP Lett. **46**, 194 (1987)].

[6]J. D. Jorgensen, B. W. Veal, W. K. Kwok, G. W. Crabtree, A. Umezawa, L. J. Nowicki, and A. P. Paulikas, Phys. Rev. B **36**, 5731 (1987).

[7]R. J. Cava, B. Batlogg, C. H. Chen, E. A. Rietman, S. M. Zakurak, and D. Werder, Nature (London) **329**, 423 (1987).

[8]R. J. Cava, Science **247**, 656 (1990).

[9]S. B. Borisov, I. L. Lyubchanskiĭ, and V. L. Sobolev, Fiz. Tverd. Tela (Leningrad) **31**, 158 (1989) [Sov. Phys. Solid State **31**, 1565 (1989)].

[10]P. Guyot-Sionnest, W. Chen, and Y. R. Shen, Phys. Rev. B **33**, 8254 (1986).

[11]J. S. Horwitz, K. S. Grabowski, D. B. Chrisey, and R. E. Leuchtner, Appl. Phys. Lett. **59**, 1565 (1991).

[12]M. Ohkubo, T. Kachi, T. Hioki, and J. Kawamoto, Appl. Phys. Lett. **55**, 899 (1989).

[13]J. H. Claassen, M. E. Reeves, and R. J. Soulen, Jr., Rev. Sci. Instrum. **62**, 992 (1991).

[14]D. Guidotti, T. A. Driscoll, and H. J. Garritsen, Solid State Commun. **46**, 337 (1983).

[15]H. W. K. Tom, T. F. Heinz, and Y. R. Shen, Phys. Rev. Lett. **51**, 1983 (1983).

[16]M. E. Parks, A. Navrotsky, K. Mocala, E. Takayama-Muromachi, A. Jacobson, and P. K. Davies, J. Solid State Chem. **79**, 53 (1989).

[17]H. W. K. Tom, C. M. Mate, X. D. Zhu, J. E. Crowell, T. F. Heinz, G. A. Somorjai, and Y. R. Shen, Phys. Rev. Lett. **52**, 348 (1984).

[18]H. W. K. Tom, C. M. Mate, X. D. Zhu, J. E. Crowell, Y. R. Shen, and G. A. Somorjai, Surf. Sci. **172**, 466 (1986).

[19]P. M. Horn, D. T. Keane, G. A. Held, J. L. Jordan-Sweet, D. L. Kaiser, and F. Holtzberg, Phys. Rev. Lett. **59**, 2772 (1987).

[20]A. I. Golovashkin, O. M. Ivanenko, G. I. Leĭtus, K. V. Mitsen, O. G. Karpinskiĭ and V. F. Shamraĭ, Pis'ma Zh. Eksp. Teor. Fiz. **46**, 325 (1987) [JETP Lett. **46**, 410 (1987)].

[21]R. Srinivasan, K. S. Girirajan, V. Ganesan, V. Radhakrishnan, and G. V. Subba Rao, Phys. Rev. B **38**, 889 (1988).

[22]B. I. Choi, Z. M. Zhang, M. J. Flik, and T. Siegrist (unpublished).

[23]S. V. Govorkov, N. I. Koroteev, I. L. Shumay, and V. V. Yakovlev, J. Opt. Soc. Am. B **8**, 1023 (1991).

[24]E. D. Specht, C. J. Sparks, A. G. Dhere, J. Brynestad, O. B. Cavin, D. M. Kroeger, and H. A. Oye, Phys. Rev. B **37**, 7426 (1988).

[25]C. P. Poole, Jr., T. Datta, and H. A. Farach, *Copper Oxide Superconductors* (Wiley, New York, 1988), p. 109.

[26]P. M. Grant, R. B. Beyers, E. M. Engler, G. Lim, S. S. P. Parkin, M. L. Ramirez, V. Y. Lee, A. Nazzal, J. E. Vazquez, and R. J. Savoy, Phys. Rev. B **35**, 7242 (1987).

[27]J. van den Berg, C. J. van der Beek, P. H. Kes, J. A. Mydosh, G. J. Nieuwenhuys, and L. J. de Jongh, Solid State Commun. **64**, 699 (1987).

[28]J. van der Berg, C. J. van der Beek, P. H. Kes, G. J. Neiuwenhuys, J. A. Mydosh, H. W. Zandbergen, F. P. F. van Berkel, R. Steens, and D. J. W. Ijdo, Europhys. Lett. **4**, 737 (1987).

[29]R. M. Hazen, L. W. Finger, R. J. Angel, C. T. Prewitt, N. L. Ross, H. K. Mao, C. G. Hadidiacos, P. H. Hor, R. L. Meng, and C. W. Chu, Phys. Rev. B **35**, 7238 (1987); **36**, 3966(E) (1987).

[30]N. Bloembergen and Y. R. Shen, Phys. Rev. **141**, 298 (1966).

[31]N. Bloembergen, R. K. Chang, and C. H. Lee, Phys. Rev. Lett. **16**, 986 (1966).

[32]W. Heuer, L. Schröder, and H. Zacharias, Chem. Phys. Lett. **135**, 299 (1987).

[33]S. Tajima, H. Ishii, T. Nakahashi, T. Takagi, S. Uchida, M. Seki, S. Suga, Y. Hidaka, M. Suzuki, T. Murakami, K. Oka, and H. Unoki, J. Opt. Soc. Am. B **6**, 475 (1989).

[34]M. Garriga, J. Humlíček, J. Barth, R. L. Johnson, and M. Cardona, J. Opt. Soc. Am. B **6**, 470 (1989).

[35]I. Fugol, G. Saemann-Ischenko, V. Samovarov, Y. Rybalko, V. Zhuravlev, Y. Ströbel, B. Holzäpfel, and P. Berberich, Solid State Commun. **80**, 201 (1991).